

Supporting Information

Origin of Free Energy Barriers of Decarboxylation and the Reverse Process of CO₂ Capture in Dimethylformamide and in Water

Shaoyuan Zhou,^{1,2} Bach T. Nguyen,³ John P. Richard,^{4*} Ronald Kluger,^{5*}
and Jiali Gao^{1,3*}

¹Institute of Systems and Physical Biology, Shenzhen Bay Laboratory, Shenzhen
581055, China

²Institute of Theoretical Chemistry, Jilin University, Changchun 100231, China

³Department of Chemistry and Supercomputing Institute, University of Minnesota,
Minneapolis, MN 55455, USA

⁴Department of Chemistry, State University of New York at Buffalo, Buffalo, NY
47907, USA

⁵Department of Chemistry, University of Toronto, Toronto, Ontario M5S 3H6,
Canada

This supporting information contains a brief description of the dual-level combined quantum mechanical and molecular mechanical (QM/MM) method used in the present study and simulation details, summary of computed and experimental energies, a list of the reaction schemes, figures presenting the computed potentials of mean force for all reactions examined in this study and a list of optimized stationary and transition structures (29 pages).

Combined QM/MM with dual-level QM models.

A dual-level approach is used in the present simulation study, in which (1) an efficient QM/MM method is used to model solvation effects, and (2) a high-level quantum chemical method is employed to achieve the required accuracy.¹⁻⁴ The method which can achieve high accuracy with a balance in computational efficiency has been developed in a variety of different ways in recent studies.⁵⁻¹⁰ A brief summary of the key concepts is given below.

The standard effective Hamiltonian of a combined QM/MM potential is given by

$$H_{eff} = H_X + H_{Xs} + V_{ss} \quad (S1)$$

where H_X is the electronic Hamiltonian of the solute molecule, H_{Xs} is the interaction Hamiltonian between the solute and all solvent molecules, and V_{ss} denotes the potential energy function for the solvent system. Equation S1 is typically used directly in combined QM/MM calculations,¹¹ but its efficiency is limited by the costs and unfavorable scaling of high-level QM methods. An alternative, equivalent representation can be used by separating the electronic energy for the solute (the first term of eq. 1) into a constant value, its energy in the gas phase (E_X^o) and a net solute-solvent interaction term.^{2, 4, 12}

$$H_{eff} = E_X^o + \Delta H_{Xs}^{tr} + V_{ss} \quad (S2)$$

where the second terms, $\Delta H_{Xs}^{tr} = (H_X + H_{Xs}) - E_X^o$, defines the interaction, or transfer energy for the solute X from the gas phase into solution.

Nothing has changed, but eq. S2 provides a convenient way of separating a QM/MM potential into a high-level (HL) description of the intrinsic properties of the “QM” molecule in the gas phase (E_X^o), and a lower scaling (LS) model (ΔH_{Xs}^{int}). Here, we make the approximation that a high-level quantum chemical model is used to describe the intrinsic reactivity of the solute molecule itself, whereas solute-solvent polarization interactions can be described by a computationally more efficient quantum chemical technique such as lower-scaling semiempirical methods and density functional theory. The total energy of a dual-level QM/MM potential is given by

$$E_{tot} = E_X^{o,HL} + \Delta E_{Xs}^{tr,LS} + V_{ss} \quad (S3)$$

In eq S3, the superscripts emphasize the relative levels of theory used to determine the corresponding energies. The second term is the transfer energy, computed using a different (LS) QM method from the first term (HL):

$$\Delta E_{Xs}^{tr,LS} = \langle \Psi_X | \Delta H_{Xs}^{tr,LS} | \Psi_X \rangle \quad (S4)$$

where Ψ_X is the polarized wave function of the solute molecule in solution, and

$\Delta H_{Xs}^{tr,LS}$ is the transfer-interaction Hamiltonian. Dual-level approaches have been applied to many systems,^{5-10, 13-15} and a most successful method is that developed by the Moliner and Tunon groups for enzymatic reactions.¹⁶⁻¹⁸ Eqs. S3 and S4 emphasize that a dual level QM/MM approach differs from a single level QM/MM calculation. Condensed-phase simulations are carried out using an LS-QM(AM1)/MM approach in which the most critical quantity is the solute-solvent interaction term. The M06-2X/aug-cc-pVTZ density functional theory is used for the HL energies for the solute molecules.

Validation of QM/MM interactions

Combined QM/MM models contain empirical parameters to model short-range exchange repulsion and long-range dispersion interactions between the two regions. They are described by the Lennard-Jones terms.

$$\Delta H_{Xs}^{vdw} = \sum_q^{QM} \sum_m^{MM} 4\epsilon_{qm} \left[\left(\frac{\sigma_{qm}}{R_{qm}} \right)^{12} - \left(\frac{\sigma_{qm}}{R_{qm}} \right)^6 \right] \quad (S5)$$

where q and m denote, respectively, atoms in the QM and MM regions, using standard combining rules such that $\epsilon_{qm} = (\epsilon_q \epsilon_m)^{1/2}$ and $\sigma_{qm} = (\sigma_q + \sigma_m) / 2$. The van der Waals parameters for atoms in the MM region (σ_m and ϵ_m) are taken directly from the OPLS force field and the three-point charge TIP3P model for water. The parameters for the ‘‘QM’’ atoms are different for each specific QM/MM combination, which must be optimized to accurately describe solute-solvent interactions.^{19, 20}

In a separate work, we have optimized these parameters by examining a set of 34 bimolecular complexes between organic acids and a water molecule at different conformations, having the target of interactions represented by the Minnesota functional M06-2X and the aug-cc-pVTZ basis set.²¹ The results are used as a consistent target for modeling the relative interaction energies due to steric and substituent effects on hydrogen-bonding complexes. Then, the Lennard-Jones parameters for atoms represented by the LS Austin Model 1 (AM1),²² were optimized in QM/MM calculations to best reproduce the full DFT binding energies. Starting from the Lennard-Jones parameters generated by the CHARMM general force field for small molecules, we found that a single set of parameters for most elements is sufficient, consistent with early studies of similar complexes with little adjustments.²³ We emphasize that the

quality of the presently optimized LS-QM/MM model can provide results for hydrogen-bonding interaction energies as good as full DFT calculations at the M06-2X/aug-cc-pVTZ level. The results from the full QM M06-2X optimizations are in good accord with data obtained by using the QM/MM method with a root-mean-square deviation of 0.78 kcal/mol for an energy range over 25 kcal/mol. Full details of this work will be reported elsewhere.

Computational details

We carried out molecular dynamics simulations to determine the potentials of mean force along the CO₂ dissociation coordinate for a set of 11 organic acids (Table S1) in water and in DMF, employing a dual-level QM/MM potential^{2, 11} to yield results at a quality of density functional theory with the M06-2X/aug-cc-pVTZ functional,²¹ in which solvation effects are determined from an optimized low-scaling QM/MM potential combining AM1²² and TIP3P²⁴ for treating solute-solvent interactions. All simulations were executed in the isothermal-isobaric ensemble at 25 °C and 1 atm, containing one carboxylate and 4720 to 6485 water molecules in cubic boxes, or 620 DMF molecules (42×42×42 Å³). Periodic boundary conditions were used along with the particle mesh-Ewald method to treat long-range electrostatic interactions in the QM/MM potential with a real-space distance of 12 Å.²⁵ The latter is also used to switch off the van der Waals potential. Potassium ions were added to keep charge neutrality. For each PMF, the calculation was divided into 20 separate simulations to span the reaction coordinate for a cumulative of 1 ns at an integration step of 1 fs.^{26, 27}

For the nine reactions where experimental data are available, the root-mean-square-errors (RMSE) between experiment and computation are 4.4 and 6.1 kcal/mol, respectively, for the barrier height and reaction free energy (Table S2). The agreement is good in view of the large span of rates and free energies. No systematic errors were observed as the mean-signed-errors (MSE) are smaller (0.3 and 1.2 kcal/mol) than unsigned errors and RMSE.²⁸

References

1. Gao, J., Origin of the solvent effects on the barrier to amide isomerization from the combined QM/MM Monte Carlo simulations. *Proc. Ind. Acad. Sci.* **1994**, *106* (2), 507-519.
2. Gao, J., Enzymatic Kinetic Isotope Effects from Path-Integral Free Energy Perturbation Theory. *Methods Enzymol.* **2016**, *577*, 359-388.
3. Vreven, T.; Morokuma, K.; Farkas, O.; Schlegel, H. B.; Frisch Michael, J., Geometry optimization with QM/MM, ONIOM, and other combined methods. I. Microiterations and constraints. *J Comput Chem* **2003**, *24* (6), 760-9. FIELD Reference Number: FIELD Journal Code:9878362 FIELD Call Number:.
4. Marti, S.; Moliner, V.; Tunon, I., Improving the QM/MM Description of Chemical Processes: A Dual Level Strategy To Explore the Potential Energy Surface in Very Large Systems. *J. Chem. Theory Comput.* **2005**, *1* (5), 1008-1016.
5. Konig, G.; Hudson, P. S.; Boresch, S.; Woodcock, H. L., Multiscale Free Energy Simulations: An Efficient Method for Connecting Classical MD Simulations to QM or QM/MM Free Energies Using

- Non-Boltzmann Bennett Reweighting Schemes. *Journal of Chemical Theory and Computation* **2014**, *10* (4), 1406-1419.
6. Nam, K., Acceleration of Ab Initio QM/MM Calculations under Periodic Boundary Conditions by Multiscale and Multiple Time Step Approaches. *Journal of Chemical Theory and Computation* **2014**, *10* (10), 4175-4183.
7. Pan, X. L.; Li, P. F.; Ho, J. M.; Pu, J. Z.; Mei, Y.; Shao, Y. H., Accelerated computation of free energy profile at ab initio quantum mechanical/molecular mechanical accuracy via a semi-empirical reference potential. II. Recalibrating semi-empirical parameters with force matching. *Physical Chemistry Chemical Physics* **2019**, *21* (37), 20595-20605.
8. Giese, T. J.; York, D. M., Development of a Robust Indirect Approach for MM -> QM Free Energy Calculations That Combines Force-Matched Reference Potential and Bennett's Acceptance Ratio Methods. *Journal of Chemical Theory and Computation* **2019**, *15* (10), 5543-5562.
9. Doron, D.; Major, D. T.; Kohen, A.; Thiel, W.; Wu, X., Hybrid quantum and classical simulations of the dihydrofolate reductase catalyzed hydride transfer reaction on an accurate semi-empirical potential energy surface. *J Chem Theory Comput* **2011**, *7* (10), 3420-37.
10. Liang, S.; Roitberg, A. E., AM1 specific reaction parameters for reactions of hydroxide ion with halomethanes in complex environments: development and testing. *J Chem Theory Comput* **2013**, *9* (10), 4470-80.
11. Gao, J., Hybrid Quantum Mechanical/Molecular Mechanical Simulations: An Alternative Avenue to Solvent Effects in Organic Chemistry. *Acc. Chem. Res.* **1996**, *29* (6), 298-305.
12. Roca, M.; Navas-Yuste, S.; Zinovjev, K.; Lopez-Esteba, M.; Gomez, S.; Fernandez, F. J.; Vega, M. C.; Tunon, I., Elucidating the Catalytic Reaction Mechanism of Orotate Phosphoribosyltransferase by Means of X-ray Crystallography and Computational Simulations. *ACS Catal* **2020**, *10* (3), 1871-1885.
13. Lu, X. Y.; Fang, D.; Ito, S.; Okamoto, Y.; Ovchinnikov, V.; Cui, Q., QM/MM free energy simulations: recent progress and challenges. *Molecular Simulation* **2016**, *42* (13), 1056-1078.
14. da Silva, G. C. Q.; Cardozo, T. M.; Amarante, G. W.; Abreu, C. R. A.; Horta, B. A. C., Solvent effects on the decarboxylation of trichloroacetic acid: insights from ab initio molecular dynamics simulations. *Physical Chemistry Chemical Physics* **2018**, *20* (34), 21988-21998.
15. Gao, J., An automated procedure for simulating chemical reactions in solution. application to the decarboxylation of 3-carboxybenzoxazole in Water. *Journal of The American Chemical Society* **1995**, *117*, 8600-8607.
16. De Raffe, D.; Marti, S.; Moliner, V., QM/MM Theoretical Studies of a de Novo Retro-Aldolase Design. *ACS Catalysis* **2019**, *9* (3), 2482-2492.
17. Marti, S.; Moliner, V., Improving the QM/MM description of chemical processes: a dual level strategy to explore the potential energy surface in very large systems. *Journal of Chemical Theory and Computation* **2005**, *1*, 1008-1016.
18. Ruiz-Permi, J. J.; Garcia-Viloca, M.; Bhattacharyya, S.; Gao, J.; Truhlar, D. G.; Tunon, I. a., Critical Role of Substrate Conformational Change in the Proton Transfer Process Catalyzed by 4-Oxalocrotonate Tautomerase. *Journal of The American Chemical Society* **2009**, *131*, 2687-2698.
19. Gao, J.; Xia, X., A priori evaluation of aqueous polarization effects through monte carlo QM-MM simulation. *Science* **1992**, *258*, 631-634.
20. Freindorf, M.; Gao, J., Optimization of the Lennard-Jones parameters for a combined Ab initio

quantum mechanical and molecular mechanical potential using the 3-21G basis set. *Journal of Computational Chemistry* **1996**, *17*, 386-395.

21. Zhao, Y.; Truhlar, D. G., M06 DFT functionals. *Theor. Chem. Acc.* **2008**, *120*, 215.
22. Dewar, M. J. S.; Zoebisch, E. G.; Healy, E. F.; Stewart, J. J. P., Development and use of quantum mechanical molecular models. 76. AM1: a new general purpose quantum mechanical molecular model. *J. Am. Chem. Soc.* **1985**, *107* (13), 3902-9.
23. Gao, J.; Xia, X., A prior evaluation of aqueous polarization effects through Monte Carlo QM-MM simulations. *Science* **1992**, *258* (5082), 631-5.
24. Jorgensen, W. L.; Chandrasekhar, J.; Madura, J. D.; Impey, R. W.; Klein, M. L., Comparison of simple potential functions for simulating liquid water. *J. Chem. Phys.* **1983**, *79* (2), 926-35.
25. Nam, K.; Gao, J.; York, D. M., An Efficient Linear-Scaling Ewald Method for Long-Range Electrostatic Interactions in Combined QM/MM Calculations. *J. Chem. Theory Comput.* **2005**, *1* (1), 2-13.
26. Brooks, B. R.; Brooks, C. L.; Mackerell, A. D.; Nilsson, L.; Petrella, R. J.; Roux, B.; Won, Y.; Archontis, G.; Bartels, C.; Boresch, S.; Caffisch, A.; Caves, L.; Cui, Q.; Dinner, A. R.; Feig, M.; Fischer, S.; Gao, J.; Hodoseck, M.; Im, W.; Kuczera, K.; Lazaridis, T.; Ma, J.; Ovchinnikov, V.; Paci, E.; Pastor, R. W.; Post, C. B.; Pu, J. Z.; Schaefer, M.; Tidor, B.; Venable, R. M.; Woodcock, H. L.; Wu, X.; Yang, W.; York, D. M.; Karplus, M., CHARMM: The Biomolecular Simulation Program. *J. Comput. Chem.* **2009**, *30* (10), 1545-1614.
27. MacKerell, A. D., Jr.; Bashford, D.; Bellott, M.; Dunbrack, R. L.; Evanseck, J. D.; Field, M. J.; Fischer, S.; Gao, J.; Guo, H.; Ha, S.; Joseph-McCarthy, D.; Kuchnir, L.; Kuczera, K.; Lau, F. T. K.; Mattos, C.; Michnick, S.; Ngo, T.; Nguyen, D. T.; Prodhom, B.; Reiher, W. E., III; Roux, B.; Schlenkrich, M.; Smith, J. C.; Stote, R.; Straub, J.; Watanabe, M.; Wiorkiewicz-Kuczera, J.; Yin, D.; Karplus, M., All-Atom Empirical Potential for Molecular Modeling and Dynamics Studies of Proteins. *J. Phys. Chem. B* **1998**, *102* (18), 3586-3616.
28. Lewis, C. A.; Wolfenden, R., Orotic Acid Decarboxylation in Water and Nonpolar Solvents: A Potential Role for Desolvation in the Action of OMP Decarboxylase. *Biochemistry* **2009**, *48* (36), 8738-8745.

Figure S1. Computed potential of mean force for the eleven anions in gas phase(red), in aqueous solution(black) and in DMF(green) along the eleven decarboxylation reaction coordinates.

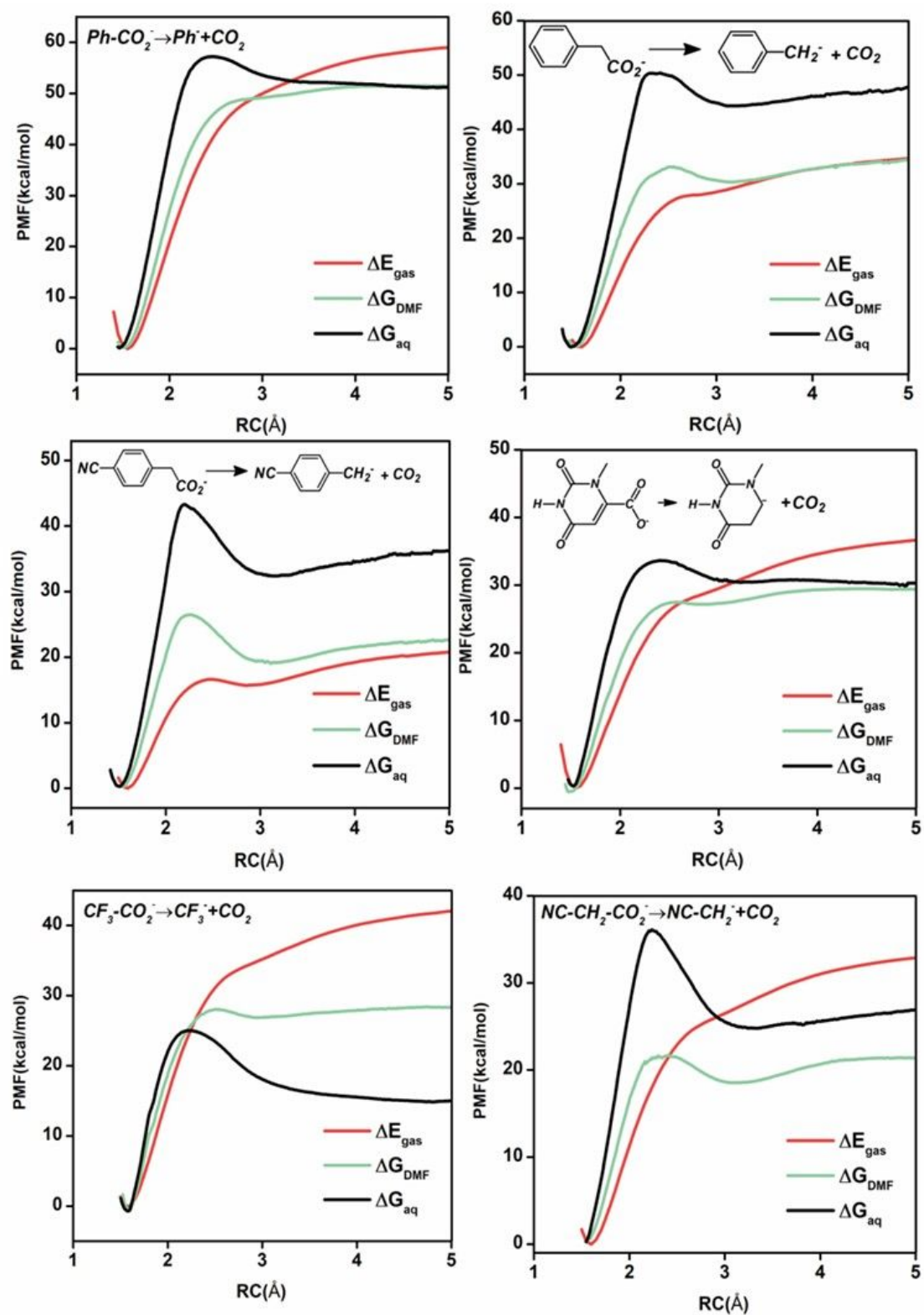


Figure S1. Continued.

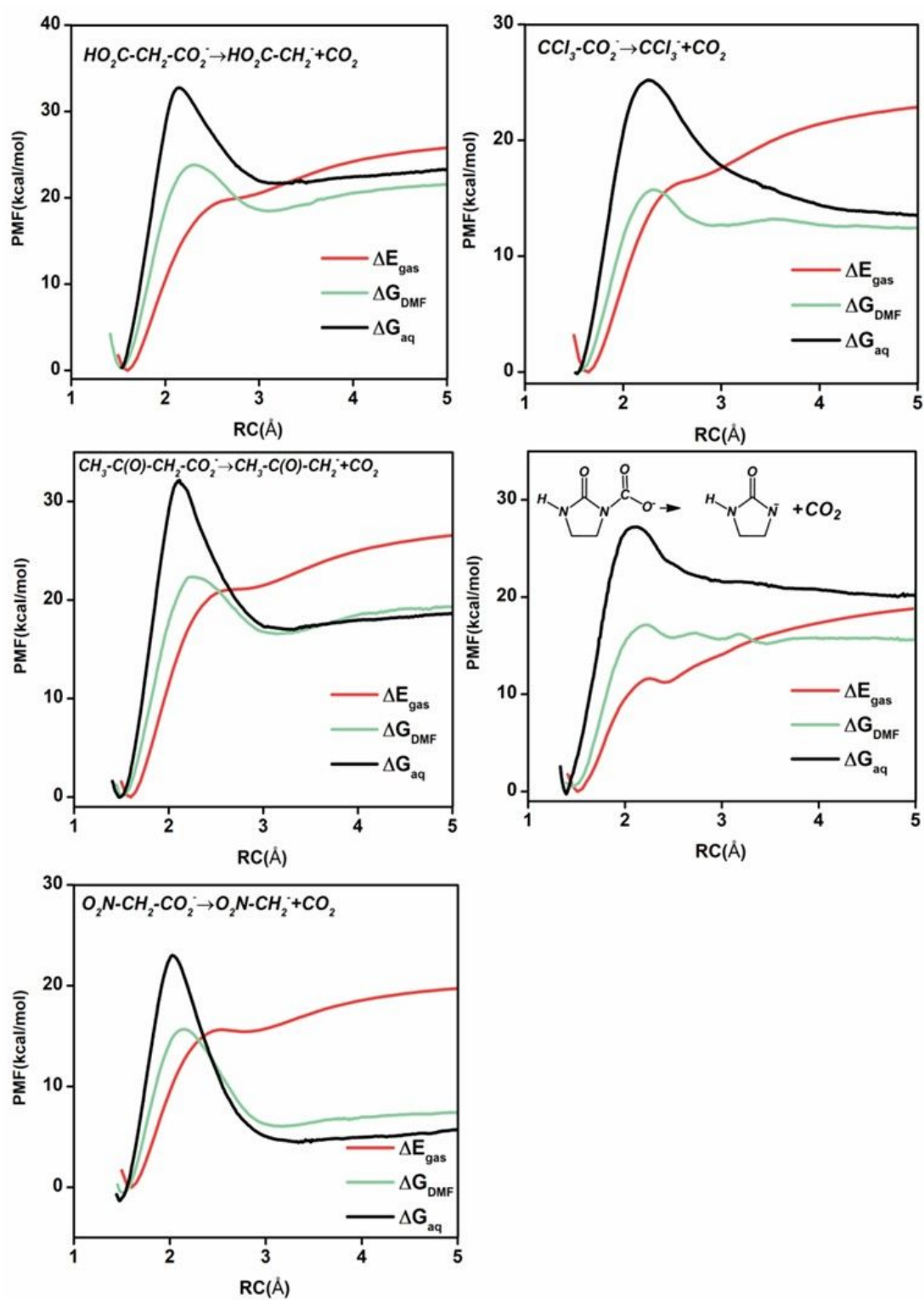


Figure S2. Relative free energies (kcal/mol) of nucleophilic addition of *p*-NC-C₆H₄CH₂⁻ to dimethylformamide computed using M06-2x(SMD)/aug-cc-pVTZ//B3LYP/aug-cc-pVDZ. Total energies and the coordinates for the optimized transition structure are given below.

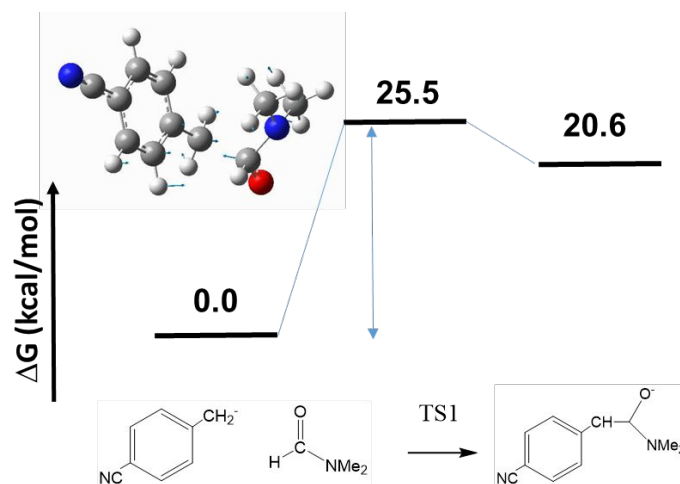


Figure S3. Relative free energies (kcal/mol) associated with the disproportionation reaction of *p*-NC-C₆H₄CH₂CO₂⁻. Solvation model corresponding to DMSO was used, and all calculations were performed using M06-2x(SMD)/aug-cc-pVTZ//B3LYP/aug-cc-pVDZ. Total energies and the coordinates for the optimized transition structure are given below.

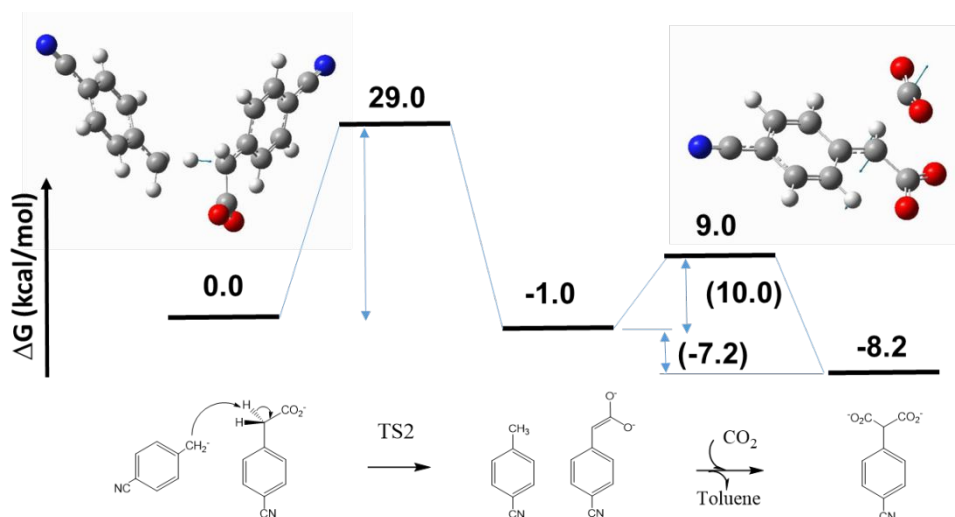


Table S1. Decarboxylation reactions of 11 anions in DMF and details of QM/MM simulation models.

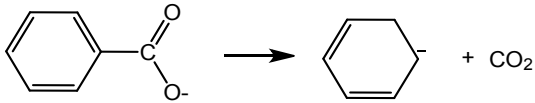
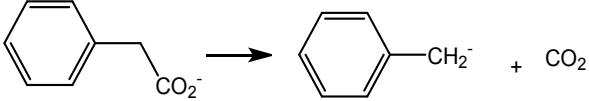
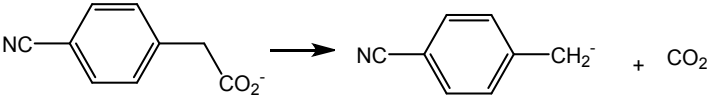
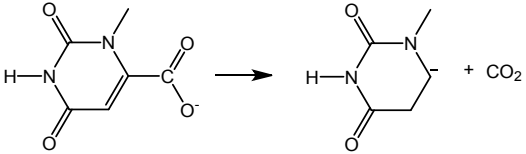
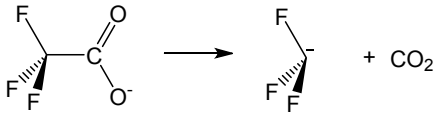
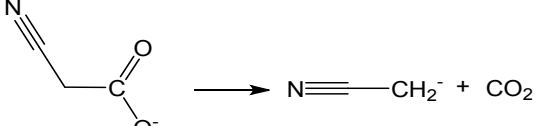
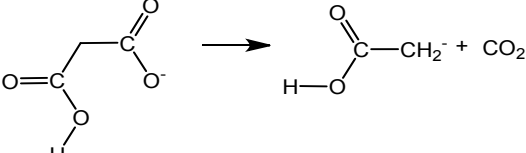
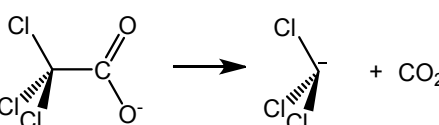
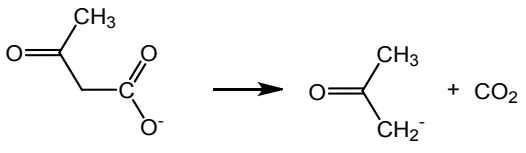
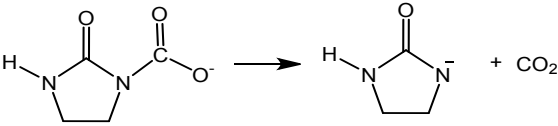
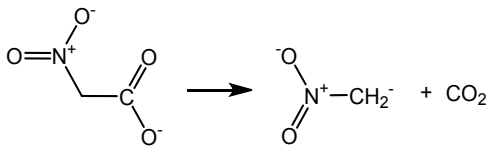
NO.	Reactions	Total Atoms
1		7466
2		7469
3		7470
4		7433
5		7459
6		7364
7		7462
8		7459
9		7464
10		7466
11		7461

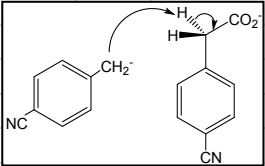
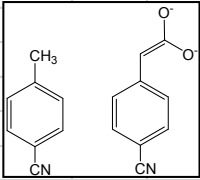
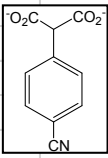
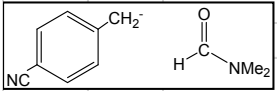
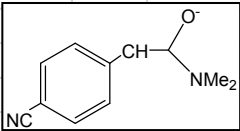
Table S2. Computed and experimental free energies of activation and reaction for decarboxylation reactions in aqueous solution and computed values in dimethylformamide.

Carboxylate	Aqueous solution				DMF	
	ΔG_{expt}^\ddagger	ΔG_{calc}^\ddagger	ΔG_{rxn}^{expt}	ΔG_{rxn}^{calc}	ΔG_{calc}^\ddagger	ΔG_{rxn}^{calc}
Benzoate	55.4	57.3	49.7	51.1	49.2	51.5
Phenylacetate	-	50.6	-	47.8	33.2	34.4
<i>p</i> -Cyano-phenylacetate	-	43.4	-	36.2	26.3	22.6
<i>N</i> -Methyl orotate	38.6	33.7	32.6	30.1	27.6	29.5
Trifluoromethyl acetate	34.2	25.1	29.1	15.1	28.1	28.4
Cyanoacetate	33.2	36.0	20.1	27.8	21.7	21.5
Malonate monoanion	29.4	32.7	21.3	23.5	23.8	21.6
Trichloroacetate	28.4	25.3	13.5	13.6	15.9	12.5
Acetoacetate	26.3	31.9	10.8	18.9	22.4	19.3
Oxoimidazolidine-1-carboxylate	23.2	27.3	14.6	20.0	17.2	15.7
Nitroacetate	21.0	22.9	3.1	5.8	15.7	7.4
MSE		0.3		1.2		
RMSE		4.6		6.4		

Table S3. Computed energies for the proton abstraction of DMSO by NCCH₂ and by *p*-NC-C₆H₄CH₂. All structures and energies are computed with structures optimized M06-2X/aug-cc-pVTZ, except the transition state for the proton transfer between DMSO and *p*-NC-C₆H₄CH₂ which was optimized at the B3LYP/aug-cc-pVDZ (energies are determined using M06-2X/aug-cc-pVTZ single-point calculations). Energies are given in hartree. Coordinates for the transition structures are given below.

	M06-2X/aug-cc-pVTZ//M06-2X/aug-cc-pVTZ		
	E(elec)	G(thermal corr)	SMD total energy
NCCH2(-)	-132.14380	-132.13736	-132.24067
NCC6H4CH2(-)	-363.20373	-363.12239	-363.27972
CH3SOCH2(-)	-552.58263	-552.54478	-552.67274
NCCH3	-132.69687	-132.72541	-132.75641
<i>p</i> -cyanotoluene	-363.78514	-363.68955	-363.79591
DMSO	-553.19207	-553.14033	-553.20498
TS4 for PT of NCCH2(-)/DMSO	-685.34141	-685.26996	-685.41524
TS5 for PT of <i>p</i> NCbenzyl(-)/DMSO	-916.48594	-916.34435	-916.44362
	optimized at B3LYP/aug-cc-pVDZ		SP=-916.37395

Table S4. Computed energies for the nucleophilic addition of *p*-NC-C₆H₄CH₂⁻ to the carbonyl group of DMF and the disproportionation reaction of *p*-NC-C₆H₄CH₂CO₂⁻. These two reactions were considered as potential competitive pathways to CO₂ recombination. As can be seen, both processes have substantially higher free energy barriers than the carboxylation reaction with nucleophilic addition to CO₂. All structures were optimized using B3LYP/aug-cc-pVDZ along with vibrational frequency calculations, and energetic results are computed using M06-2X/aug-cc-pVTZ. Energies are given in hartree. Coordinates for the transition structures are given below.

	B3LYP/aug-cc-pVDZ optimized		SP with SMD(DMSO)	
	E(elec)	G(thermal corr)	M06-SMD/ACCT	
	p-cyanobenzyl ion	-363.26876	-363.18887	-363.27798
	p-cyanophenylacetate	-551.91529	-551.82531	-551.91403
	TS for PT	-915.09392	-914.90989	-915.15994
	p-cyanotoluene	-363.85039	-363.75645	-363.79434
	p-cyanophenyldienolate	-551.22509	-551.14695	-551.40142
	co2	-188.61421	-188.62335	-188.59544
	TS for dienolate addition to CO ₂	-739.84726	-739.76427	-739.99493
	dicarboxylate dianion	-739.86740	-739.78014	-740.02661
	p-cyanobenzyl ion	-363.26876	-363.18887	-363.27798
	DMF	-248.54529	-248.47295	-248.50682
	TS for addition to DMF	-611.79677	-611.62368	-611.76499
	Product of addition	-611.79677	-611.62480	-611.77175

Optimized geometries using M06-2X/aug-cc-pVTZ.

Benzene, -232.2245

6	0	0.98751	-0.97583	0.00000
6	0	1.33887	0.36728	-0.00001
6	0	0.35136	1.34313	0.00001
6	0	-0.98752	0.97583	-0.00001
6	0	-1.33886	-0.36728	0.00000
6	0	-0.35136	-1.34313	0.00002
1	0	1.75683	-1.73597	0.00000
1	0	2.38186	0.65336	-0.00002
1	0	-1.75683	1.73598	-0.00002
1	0	-2.38185	-0.65336	0.00000
1	0	0.62508	2.38942	0.00000
1	0	-0.62508	-2.38942	0.00003

C6H5(-), -231.57521

6	0	1.19258	0.64638	0.00004
6	0	1.17010	-0.74972	0.00000
6	0	0.00001	-1.54273	-0.00001
6	0	-1.17010	-0.74972	0.00001
6	0	-1.19259	0.64637	-0.00004
6	0	0.00000	1.36245	0.00001
1	0	2.14003	1.18144	0.00008
1	0	2.14376	-1.24394	0.00006
1	0	-2.14374	-1.24397	-0.00009
1	0	-2.14003	1.18143	-0.00010
1	0	-0.00002	2.44686	0.00000

C6H5CH3, -271.53535

6	0	1.19355	-1.19840	0.00202
6	0	-0.19390	-1.19521	-0.00887
6	0	-0.90766	-0.00002	-0.01171
6	0	-0.19391	1.19520	-0.00887
6	0	1.19351	1.19842	0.00202
6	0	1.89309	0.00001	0.00847
1	0	1.72904	-2.13836	0.00185
1	0	-0.73322	-2.13461	-0.01855
1	0	-0.73328	2.13458	-0.01854
1	0	1.72901	2.13838	0.00185
1	0	2.97443	0.00003	0.01439
6	0	-2.41126	-0.00001	0.00941
1	0	-2.81190	0.88313	-0.48620
1	0	-2.81192	-0.88357	-0.48543

1	0	-2.78266	0.00046	1.03573
---	---	----------	---------	---------

C6H5CH2(-), -270.91754

6	0	-1.13268	-1.19283	0.00000
6	0	0.24256	-1.20605	-0.00002
6	0	1.03382	0.00000	0.00000
6	0	0.24256	1.20605	-0.00001
6	0	-1.13267	1.19284	0.00000
6	0	-1.86952	0.00000	0.00002
1	0	-1.66045	-2.14262	0.00000
1	0	0.76585	-2.15677	-0.00003
1	0	0.76585	2.15676	-0.00003
1	0	-1.66045	2.14262	0.00000
1	0	-2.95061	0.00000	0.00004
6	0	2.41507	0.00000	-0.00003
1	0	2.97249	0.92749	0.00015
1	0	2.97251	-0.92748	0.00014

p-CN-C6H4-CH3, -363.78514

6	0	0.41192	1.20592	-0.00319
6	0	-0.97139	1.19703	-0.00982
6	0	-1.68433	0.00011	-0.01054
6	0	-0.97145	-1.19691	-0.00985
6	0	0.41181	-1.20591	-0.00321
6	0	1.10945	0.00000	0.00115
1	0	0.95786	2.13861	-0.00458
1	0	-1.50901	2.13637	-0.01762
1	0	-1.50915	-2.13621	-0.01767
1	0	0.95769	-2.13863	-0.00462
6	0	-3.18571	-0.00004	0.01401
1	0	-3.54968	-0.00551	1.04285
1	0	-3.58779	0.88620	-0.47329
1	0	-3.58765	-0.88130	-0.48243
6	0	2.54401	-0.00007	0.00481
7	0	3.69169	-0.00006	0.00817

p-CN-C6H4-CH2(-), -363.20373

6	0	-0.33884	1.20761	-0.00001
6	0	1.02302	1.21575	0.00001
6	0	1.81232	-0.00004	0.00001
6	0	1.02292	-1.21576	0.00001
6	0	-0.33893	-1.20751	0.00000
6	0	-1.08090	0.00008	-0.00001
1	0	-0.87978	2.14714	-0.00001

1	0	1.55023	2.16295	0.00001
1	0	1.55006	-2.16300	0.00001
1	0	-0.87995	-2.14699	-0.00001
6	0	3.17868	-0.00009	0.00003
1	0	3.73663	0.92675	0.00003
1	0	3.73656	-0.92697	0.00003
6	0	-2.48987	0.00016	-0.00002
7	0	-3.64916	-0.00016	-0.00002

N-methyl-Uracil, -338.27267

6	0	0.64008	-0.86103	0.00052
6	0	0.18439	1.49716	0.00000
6	0	-1.14653	1.33419	-0.00001
6	0	-1.70469	-0.00703	-0.00002
1	0	-1.82216	2.17242	-0.00018
1	0	0.63695	2.47902	-0.00016
8	0	-2.87824	-0.29628	-0.00027
8	0	1.41047	-1.79308	-0.00018
7	0	-0.72742	-1.00863	0.00018
7	0	1.07383	0.45610	0.00014
1	0	-1.06021	-1.96283	-0.00008
6	0	2.51593	0.66243	-0.00011
1	0	2.71104	1.73057	-0.00072
1	0	2.95836	0.20502	0.88190
1	0	2.95819	0.20404	-0.88168

N-methyl-Uracil-6(-), -453.53749

6	0	-0.65517	0.80264	-0.00019
6	0	-0.21613	-1.63135	-0.00014
6	0	1.12971	-1.34540	-0.00006
6	0	1.68293	-0.02695	-0.00010
1	0	1.85140	-2.15161	0.00008
8	0	2.86485	0.31901	0.00023
8	0	-1.43088	1.75721	0.00021
7	0	0.70331	0.97813	-0.00005
7	0	-1.05517	-0.50878	-0.00014
1	0	1.02733	1.93224	0.00017
6	0	-2.49590	-0.70169	0.00003
1	0	-2.66052	-1.77351	-0.00011
1	0	-2.94966	-0.24308	0.88040
1	0	-2.94987	-0.24279	-0.88006

F3CH, -338.27267

1	0	0.00000	-0.00002	1.42783
---	---	---------	----------	---------

6	0	-0.00002	-0.00004	0.34004
9	0	1.00770	-0.73379	-0.12853
9	0	-1.13942	-0.50565	-0.12851
9	0	0.13174	1.23946	-0.12830

F3C(-), -337.65837

6	0	-0.00002	0.00014	0.54526
9	0	-1.07744	0.63784	-0.12119
9	0	1.09145	0.61359	-0.12118
9	0	-0.01401	-1.25153	-0.12114

NCCH3, -132.74714

1	0	1.54379	-0.17250	1.00852
6	0	1.17500	0.00002	0.00004
1	0	1.54387	0.95966	-0.35465
1	0	1.54412	-0.78701	-0.65351
6	0	-0.28190	-0.00008	-0.00020
7	0	-1.42719	0.00003	0.00009

NCCH2(-), -132.14380

6	0	1.19541	-0.00004	-0.04472
1	0	1.72552	-0.92732	0.11088
1	0	1.72572	0.92712	0.11089
6	0	-0.18523	0.00015	0.00018
7	0	-1.35891	-0.00006	0.00650

HOOCCH3, -229.08936

1	0	-1.65593	-0.71044	-0.87789
6	0	-1.38820	-0.12498	0.00001
1	0	-1.91676	0.82128	-0.00035
1	0	-1.65586	-0.70967	0.87845
6	0	0.08845	0.12591	-0.00012
8	0	0.62206	1.19932	0.00000
8	0	0.79041	-1.02659	0.00004
1	0	1.72732	-0.78858	0.00014

HOOCCH2(-), -228.49067

6	0	1.39303	-0.16898	-0.00004
1	0	2.10211	0.64346	-0.00034
1	0	1.73675	-1.19127	0.00000
6	0	0.04986	0.11713	0.00024
8	0	-0.56148	1.21001	-0.00015
8	0	-0.79262	-1.02555	0.00005
1	0	-1.66338	-0.61677	-0.00006

Cl3CH, -1419.31172

1	0	0.00000	0.00000	1.53890
6	0	0.00000	0.00000	0.45843
17	0	0.00000	1.67956	-0.08411
17	0	1.45454	-0.83978	-0.08411
17	0	-1.45454	-0.83978	-0.08411

Cl3C(-), -1418.73069

6	0	0.00000	0.00000	0.72453
17	0	0.00000	1.69622	-0.08524
17	0	1.46897	-0.84811	-0.08524
17	0	-1.46897	-0.84811	-0.08524

CH3COCH3, -193.13993

1	0	-1.34636	-1.20048	-0.91449
6	0	-1.28242	-0.61058	0.00138
1	0	-2.13577	0.05716	0.06908
1	0	-1.28703	-1.31377	0.83514
6	0	0.00000	0.18592	-0.00088
6	0	1.28242	-0.61059	-0.00115
1	0	2.13585	0.05712	-0.06818
1	0	1.34530	-1.19999	0.91512
1	0	1.28801	-1.31422	-0.83451
8	0	0.00000	1.39071	0.00022

CH3COCH2(-), -192.54335

6	0	-1.19050	-0.77397	-0.00014
1	0	-2.20787	-0.40302	-0.00012
1	0	-1.02828	-1.84315	-0.00030
6	0	-0.13306	0.11069	0.00002
6	0	1.27988	-0.49115	-0.00001
1	0	1.81809	-0.12818	0.87890
1	0	1.28343	-1.58269	-0.00015
1	0	1.81817	-0.12792	-0.87877
8	0	-0.17769	1.37644	0.00016

1-Oxoimidazolidine, -302.67434

6	0	-1.33433	-0.75240	-0.14934
6	0	-1.33432	0.75241	0.14936
1	0	-2.04440	-1.29451	0.47020
1	0	-1.56460	-0.93271	-1.20292
1	0	-1.56459	0.93266	1.20295
1	0	-2.04439	1.29456	-0.47015
7	0	0.04039	-1.09587	0.17172

7	0	0.04041	1.09590	-0.17169
6	0	0.86789	-0.00004	-0.00023
8	0	2.07484	0.00000	0.00008
1	0	0.42909	1.99303	0.06520
1	0	0.42903	-1.99309	-0.06488

1-Oxoimidazolidinyl-1-(-), -302.08526

6	0	-1.30392	-0.76413	-0.10561
6	0	-1.30003	0.75003	0.17815
1	0	-2.00125	-1.29675	0.54969
1	0	-1.64757	-0.93433	-1.14131
1	0	-1.44717	0.92903	1.25391
1	0	-2.07090	1.29483	-0.37424
7	0	0.06242	-1.19703	0.08588
7	0	0.04226	1.07536	-0.26010
6	0	0.83615	-0.13295	-0.01793
8	0	2.07011	-0.01575	0.05205
1	0	0.48002	1.86720	0.18743

O2NCH3, -245.00910

1	0	-1.64931	-0.91620	-0.47977
6	0	-1.31693	-0.00220	-0.00359
1	0	-1.65114	0.89367	-0.51212
1	0	-1.61497	0.01737	1.04143
7	0	0.17373	-0.00001	-0.00956
8	0	0.72728	-1.07445	0.00244
8	0	0.72283	1.07676	0.00243

O2NCH2(-), -244.43519

6	0	1.28455	0.00000	-0.00003
1	0	1.77933	0.95345	-0.00001
1	0	1.77932	-0.95346	-0.00002
7	0	-0.04347	0.00000	0.00009
8	0	-0.68511	-1.09761	-0.00003
8	0	-0.68510	1.09761	-0.00003

Optimized transition structures for proton transfer from DMF to the product carbanions of decarboxylation reactions. Although the carbonyl proton is slightly more acidic with a gas phase basicity of 381.4 kcal/mol than the methyl proton of DMF (GB, 385.1 kcal/mol), the latter is closer to the experimental value of 392 kcal/mol. Since the six proton sites are more exposed to the carbanions, they are treated as the proton donor. All structures have been optimized using M06-2X/aug-cc-pVTZ and verified by vibrational frequency calculations, except three structures specifically indicated below for which a point closest to a saddle point along the proton transfer pathway is used to estimate the energies.

NCCH2...H...CH2N(CH3)CHO, -380.62676

1	0	-1.07293	0.21265	0.39877
6	0	0.22376	-0.19707	1.32879
1	0	0.17236	-1.27982	1.48274
1	0	0.44512	0.27541	2.29735
7	0	1.35423	0.07013	0.42921
6	0	2.16953	-0.85413	-0.07746
1	0	1.96671	-1.84917	0.35038
6	0	1.49900	1.44203	0.00445
1	0	0.60147	1.76884	-0.52463
1	0	1.62119	2.08283	0.88249
1	0	2.36703	1.53101	-0.64391
8	0	3.04948	-0.69025	-0.92742
6	0	-1.90283	0.50509	-0.52786
1	0	-1.99660	1.59059	-0.54903
1	0	-1.47530	0.15375	-1.46656
6	0	-3.18389	-0.09762	-0.30008
7	0	-4.19114	-0.60640	-0.05425

F3C...H...CH2N(CH3)CHO, -586.14947

1	0	0.73832	-0.69974	0.00013
6	0	-0.65716	-1.31994	0.00030
1	0	-0.80663	-1.94686	0.88718
1	0	-0.80672	-1.94716	-0.88634
7	0	-1.65583	-0.23767	0.00016
6	0	-2.97509	-0.44409	-0.00013
1	0	-3.20812	-1.52256	-0.00020
6	0	-1.15027	1.12071	0.00032
1	0	-0.52468	1.28663	0.87990
1	0	-0.52443	1.28676	-0.87904
1	0	-1.98527	1.81722	0.00025
8	0	-3.86775	0.40159	-0.00032
6	0	1.95621	-0.09161	-0.00004
9	0	3.03429	-0.94209	-0.00008

9	0	2.18318	0.72573	-1.08131
9	0	2.18343	0.72594	1.08104

HOOCCH₂...H...CH₂N(CH₃)CHO, -476.96274

1	0	-0.64183	0.17099	0.16921
6	0	0.71043	0.08370	1.27773
1	0	0.69544	-0.93399	1.68143
1	0	0.85500	0.78338	2.11479
7	0	1.87875	0.19305	0.39393
6	0	2.77214	-0.77034	0.17568
1	0	2.59858	-1.63710	0.83368
6	0	1.97643	1.42090	-0.35860
1	0	1.10621	1.53352	-1.00821
1	0	1.98803	2.26838	0.33267
1	0	2.88729	1.41163	-0.95226
8	0	3.69118	-0.76779	-0.65030
6	0	-1.43293	0.14635	-0.77665
1	0	-1.42462	1.14800	-1.19757
1	0	-1.06239	-0.60441	-1.46796
6	0	-2.73453	-0.21934	-0.24818
8	0	-3.20263	-1.33223	-0.10661
8	0	-3.44774	0.85846	0.21755
1	0	-4.22869	0.47309	0.63173

N-methyl-6-uracilyl...H...CH₂N(CH₃)CHO, -702.01938

6	0	2.50317	-0.94107	-0.21134
6	0	0.56207	0.30172	0.56025
6	0	1.20850	1.48134	0.39183
6	0	2.56291	1.54728	-0.08822
1	0	0.71485	2.41543	0.61739
1	0	-0.68654	0.17383	0.97959
6	0	-2.20525	0.02478	1.39589
1	0	-2.49247	0.91365	1.96657
1	0	-2.45867	-0.85366	2.01284
7	0	-3.03252	-0.01311	0.18083
6	0	-4.15951	0.68160	0.00534
1	0	-4.41850	1.26145	0.90644
6	0	-2.55484	-0.86020	-0.88736
1	0	-1.53825	-0.57430	-1.16498
1	0	-2.53266	-1.90378	-0.55607
1	0	-3.21536	-0.76806	-1.74584
8	0	-4.85558	0.72848	-1.00765
8	0	3.25336	2.53800	-0.27388
8	0	3.07269	-1.98846	-0.47611

7	0	3.10783	0.28334	-0.36009
7	0	1.21400	-0.87716	0.26162
1	0	4.05578	0.26431	-0.70373
6	0	0.53195	-2.15250	0.44854
1	0	-0.43679	-1.94331	0.89228
1	0	0.40513	-2.66051	-0.50736
1	0	1.12052	-2.79846	1.09796

C6H5...H...CH2N(CH3)CHO, -480.07736

6	0	-3.06377	1.20200	-0.03019
6	0	-1.74973	0.97991	0.37372
6	0	-1.15463	-0.28535	0.37871
6	0	-1.97450	-1.33447	-0.05175
6	0	-3.29199	-1.14372	-0.46251
6	0	-3.84449	0.13234	-0.45333
1	0	-3.48371	2.20303	-0.01814
1	0	-1.15989	1.83626	0.70268
1	0	-1.57781	-2.34801	-0.07225
1	0	-3.89233	-1.98602	-0.79238
1	0	0.16287	-0.36246	0.90274
6	0	1.54023	-0.35031	1.40016
1	0	1.82596	-1.37224	1.66821
1	0	1.73044	0.29691	2.26987
7	0	2.40208	0.08867	0.29779
6	0	3.47936	-0.56489	-0.13600
1	0	3.68337	-1.45773	0.47789
6	0	1.98889	1.30468	-0.36737
1	0	0.96236	1.19832	-0.71959
1	0	2.01984	2.13847	0.34121
1	0	2.65975	1.50692	-1.19841
8	0	4.19330	-0.27570	-1.09790
1	0	-4.86791	0.29027	-0.77180

C6H5CH2...H...CH2N(CH3)CHO, -519.39773

6	0	-3.59132	0.63908	-0.57690
6	0	-2.47418	1.22089	-0.00377
6	0	-1.49820	0.45965	0.67011
6	0	-1.72214	-0.93035	0.71519
6	0	-2.83910	-1.51275	0.13986
6	0	-3.79233	-0.73716	-0.51272
1	0	-4.31697	1.26545	-1.08279
1	0	-2.33568	2.29380	-0.06968
1	0	-0.99834	-1.55474	1.22646
1	0	-2.97104	-2.58656	0.20403

1	0	-4.66602	-1.19179	-0.96007
6	0	-0.27704	1.06640	1.17751
1	0	0.57425	1.20782	0.19847
1	0	-0.41687	2.09127	1.52187
1	0	0.22209	0.46716	1.93924
6	0	1.81427	1.33424	-0.81280
1	0	2.39840	2.20953	-0.51157
1	0	1.67223	1.36419	-1.90207
7	0	2.58858	0.13660	-0.48343
6	0	3.78591	0.13542	0.10013
1	0	4.18206	1.15834	0.20998
6	0	1.91587	-1.11801	-0.72942
1	0	0.94721	-1.12000	-0.22713
1	0	1.73321	-1.23177	-1.80229
1	0	2.53540	-1.93673	-0.37256
8	0	4.42370	-0.84208	0.50112

p-NC-C6H4CH2...H...CH2N(CH3)CHO, -611.66474

6	0	-2.91396	1.16362	-0.19957
6	0	-1.65545	1.62597	0.11245
6	0	-0.65903	0.78027	0.64059
6	0	-1.01023	-0.57238	0.82168
6	0	-2.26616	-1.04672	0.51243
6	0	-3.24138	-0.18348	-0.00011
1	0	-3.66164	1.83552	-0.59991
1	0	-1.41585	2.66922	-0.05036
1	0	-0.27020	-1.25129	1.22653
1	0	-2.51145	-2.08887	0.66867
6	0	0.69479	1.25931	0.87393
1	0	1.34494	1.19710	-0.16061
1	0	0.73098	2.31391	1.14445
1	0	1.24616	0.65708	1.59567
6	0	2.66562	1.03100	-1.28339
1	0	3.29785	1.90779	-1.11225
1	0	2.61731	0.83294	-2.36203
7	0	3.29614	-0.11684	-0.63417
6	0	4.36709	-0.05418	0.15702
1	0	4.81858	0.95131	0.14616
6	0	2.57712	-1.36246	-0.75123
1	0	1.55316	-1.23094	-0.39359
1	0	2.52382	-1.65680	-1.80334
1	0	3.08672	-2.13123	-0.17628
8	0	4.84224	-0.96076	0.84657
6	0	-4.54818	-0.66493	-0.30966

7 0 -5.60466 -1.05112 -0.55734

CH3COCH2...H...CH2N(CH3)CHO, -441.01819

1 0 -1.22851 -0.89491 -1.17803
6 0 0.92226 -1.49802 -0.00098
1 0 1.21526 -2.08238 -0.88396
1 0 1.21410 -2.08272 0.88218
7 0 1.70895 -0.24326 -0.00020
6 0 3.04312 -0.19179 0.00037
1 0 3.47526 -1.20670 0.00034
6 0 0.97375 1.00395 -0.00016
1 0 0.32988 1.05920 -0.88107
1 0 0.32828 1.05813 0.87964
1 0 1.66797 1.84290 0.00095
8 0 3.76374 0.80886 0.00088
6 0 -2.27253 -0.54980 -1.26198
1 0 -2.43733 0.07749 -2.13457
1 0 -2.89149 -1.44822 -1.31814
6 0 -2.58492 0.20058 0.00020
6 0 -2.27340 -0.55285 1.26081
1 0 -2.43778 0.07269 2.13474
1 0 -2.89349 -1.45062 1.31500
1 0 -1.22975 -0.89888 1.17630
8 0 -3.00434 1.33920 0.00143

Cl3C...H...CH2N(CH3)CHO, -1667.20799

1 0 0.13281 0.61041 0.25712
6 0 -1.25752 1.21335 0.61324
1 0 -1.42558 2.13964 0.05910
1 0 -1.29462 1.44130 1.68650
7 0 -2.32517 0.26287 0.28103
6 0 -3.55922 0.62668 -0.07505
1 0 -3.68165 1.72202 -0.03637
6 0 -1.97828 -1.14229 0.30676
1 0 -1.22047 -1.35770 -0.45015
1 0 -1.55312 -1.39666 1.27978
1 0 -2.86908 -1.73683 0.11906
8 0 -4.48283 -0.10635 -0.42432
6 0 1.32010 0.09973 -0.00804
17 0 2.58890 1.36356 0.18821
17 0 1.69739 -1.25425 1.12129
17 0 1.41372 -0.53262 -1.69240

1-Oxoimidazolidinyl-1-(-)... H...CH2N(CH3)CHO, -550.56687

6	0	3.50153	-0.77256	-0.53503
6	0	1.94253	0.78378	0.20042
1	0	0.14276	-0.55067	0.29751
6	0	-1.35853	-0.95532	0.89353
1	0	-1.40021	-0.73180	1.96728
1	0	-1.61778	-2.01007	0.75701
7	0	-2.35656	-0.13197	0.19080
6	0	-3.64711	-0.45140	0.10115
1	0	-3.88002	-1.35105	0.69647
6	0	-1.86504	1.03449	-0.51732
1	0	-1.15779	1.57120	0.11490
1	0	-1.32467	0.73348	-1.41894
1	0	-2.70300	1.67091	-0.79329
8	0	-4.52037	0.12596	-0.54803
8	0	1.52825	1.90086	0.47377
7	0	3.33303	0.47531	0.18795
1	0	3.90475	1.26343	-0.07174
7	0	1.24848	-0.32330	-0.12487
1	0	2.21035	-2.01676	0.69277
1	0	1.85287	-2.12984	-1.03682
1	0	4.35169	-1.34986	-0.17058
1	0	3.61691	-0.61355	-1.61426
6	0	2.15436	-1.44570	-0.24332

O2NCH2...H...CH2N(CH3)CHO, -492.89708

1	0	-0.79673	-0.03872	0.28157
6	0	0.69315	-1.02794	0.20040
1	0	0.69578	-1.72196	-0.64370
1	0	0.72579	-1.60490	1.13298
7	0	1.88257	-0.16484	0.11995
6	0	3.10644	-0.60221	-0.19384
1	0	3.11749	-1.69819	-0.31259
6	0	1.68818	1.25457	0.32046
1	0	1.06819	1.66853	-0.47892
1	0	1.16738	1.42231	1.26603
1	0	2.65216	1.75929	0.33180
8	0	4.12391	0.07084	-0.35374
6	0	-1.72684	0.69097	0.44948
1	0	-1.86454	0.83027	1.51577
1	0	-1.55584	1.61123	-0.09724
7	0	-2.90131	0.05068	-0.08707
8	0	-3.17007	0.22188	-1.26992
8	0	-3.53434	-0.70787	0.63806

Optimized transition structures for the nucleophilic addition of the decarboxylation anion of p-cyanophenylacetate and the disproportionation reaction of p-cyanophenylacetate. Geometries were optimized using B3LYP/aug-cc-pVDZ.

pNC-C6H5CH2(-)/DMF, RB3LYP/Aug-CC-pVDZ = -611.79677

6	2.221363	-1.116754	-0.560936
6	0.902361	-1.423525	-0.256434
6	0.127029	-0.629255	0.633388
6	0.779483	0.499381	1.198147
6	2.098837	0.812489	0.911549
6	2.848285	0.008269	0.019308
1	2.787343	-1.748169	-1.246698
1	0.443186	-2.305164	-0.705052
1	0.222369	1.133197	1.889730
1	2.573104	1.676974	1.377121
6	-1.277393	-0.955721	0.886531
1	-1.429903	-2.032218	0.998607
1	-1.698185	-0.423061	1.747703
6	-2.454331	-0.737169	-0.429862
1	-1.816727	-1.022589	-1.312848
6	4.209343	0.319680	-0.276156
7	5.324292	0.574875	-0.515335
8	-3.475843	-1.472096	-0.157096
7	-2.764151	0.702275	-0.644302
6	-3.654716	1.287231	0.327899
1	-3.133064	1.634879	1.251694
1	-4.170675	2.163104	-0.102139
1	-4.394681	0.527014	0.605076
6	-1.687091	1.569100	-1.051956
1	-1.005953	1.022540	-1.719620
1	-2.084945	2.436860	-1.608386
1	-1.085119	1.970995	-0.209827

Proton abstraction of p-cyanophenylacetate by its decarboxylation anion, RB3LYP/Aug-CC-pVDZ = -915.09392

6	-4.370914	-0.424109	0.262121
6	-3.241812	-1.097764	-0.159736
6	-2.179692	-0.445630	-0.870544
6	-2.353279	0.961695	-1.084841
6	-3.480251	1.641788	-0.665865
6	-4.533025	0.968863	0.015528
1	-5.157723	-0.962357	0.793778
1	-3.141641	-2.163211	0.053687
1	-1.563728	1.509679	-1.602883

1	-3.574054	2.711707	-0.860558
6	-0.994834	-1.144195	-1.269090
1	-0.041850	-1.213569	-0.283099
1	-1.096846	-2.224241	-1.409112
1	-0.399308	-0.662721	-2.051980
6	1.000828	-1.520087	0.661154
1	0.403389	-1.362488	1.567367
6	-5.702372	1.658075	0.425416
7	-6.673521	2.227366	0.758553
6	2.021484	-0.528103	0.472422
6	1.988725	0.701965	1.210814
6	3.089950	-0.652945	-0.478381
6	2.923402	1.704701	1.033334
1	1.191217	0.845128	1.943066
6	4.028889	0.345820	-0.653862
1	3.134274	-1.586927	-1.037803
6	3.979420	1.556919	0.093564
1	2.858526	2.622580	1.621043
1	4.833829	0.209365	-1.379509
6	1.167834	-3.012524	0.339777
8	1.930379	-3.335438	-0.620410
8	0.473758	-3.788856	1.058386
6	4.949146	2.576570	-0.086707
7	5.753494	3.419087	-0.234044

Addition to CO2 by the product enolate dianion of the above process,
RB3LYP/Aug-CC-pVDZ = -739.84726

6	2.168094	0.751063	0.997753
6	0.814520	0.671103	1.227427
6	-0.059689	-0.247943	0.514839
6	0.618807	-1.089532	-0.457469
6	1.973387	-1.005153	-0.679205
6	2.813605	-0.083378	0.030449
1	2.772870	1.463486	1.565729
1	0.363089	1.327380	1.975982
1	-0.006750	-1.801157	-0.994753
1	2.435926	-1.663529	-1.420139
6	-1.433469	-0.282581	0.778313
6	4.201475	-0.006942	-0.199071
7	5.364713	0.058554	-0.387599
6	-2.469888	-1.279359	0.309674
8	-3.624418	-1.140713	0.835336
8	-2.140316	-2.165391	-0.540447
1	-1.781185	0.356618	1.593853

6	-2.101013	1.789738	-0.724933
8	-2.154375	1.293211	-1.790985
8	-2.142380	2.588547	0.146828

Optimized transition structures for the proton abstraction by NCCH2(-) and the decarboxylation anion of p-cyanophenylacetate from DMSO. Geometries were optimized using M06-2X/aug-cc-pVTZ for NCCH2(-) and B3LYP/aug-cc-pVDZ for the latter.

NCCH2(-)/DMSO, RM062X/Aug-CC-pVTZ = -685.34141

1	-0.922403	-0.089995	0.098136
6	0.274986	-0.937016	0.368677
1	0.146662	-1.944322	-0.025485
1	0.445051	-0.959993	1.449061
6	1.423936	1.452481	0.252329
1	0.474382	1.855992	-0.093813
1	1.433666	1.370998	1.339404
1	2.258859	2.061913	-0.085284
6	-2.001914	0.759326	-0.100809
1	-1.966258	1.523111	0.675563
1	-1.867614	1.213051	-1.082693
6	-3.228173	0.032180	-0.040571
7	-4.180561	-0.621401	0.023274
16	1.653764	-0.215552	-0.415113
8	2.998545	-0.634242	0.165782

p-NCC6H4CH2(-)/DMSO, RB3LYP/Aug-CC-pVDZ = -916.48594

6	2.961649	0.610092	1.052419
6	1.677108	1.090753	0.858478
6	0.945109	0.844426	-0.339878
6	1.610258	0.059134	-1.326479
6	2.894393	-0.426565	-1.142479
6	3.604311	-0.158511	0.052457
1	3.491788	0.825990	1.980761
1	1.207898	1.683106	1.646110
1	1.088052	-0.161429	-2.259181
1	3.372034	-1.018451	-1.924129
6	-0.430412	1.269347	-0.498429
1	-1.265915	0.342068	-0.043036
1	-0.696488	2.154087	0.094890
1	-0.746872	1.378428	-1.544460
6	-2.283176	-0.684301	0.544154
1	-2.395095	-0.475392	1.621485
1	-1.892897	-1.700575	0.388570

6	-4.145916	1.210364	-0.026035
1	-4.089116	1.433684	1.047672
1	-3.382602	1.768301	-0.582401
1	-5.149936	1.433532	-0.405317
6	4.931751	-0.642131	0.240508
7	6.022013	-1.035608	0.393553
16	-3.871246	-0.599269	-0.246434
8	-5.043181	-1.232680	0.584852